


Anderson Localization Transition in Disordered Hyperbolic Lattices

Anffany Chen¹,* Joseph Maciejko², and Igor Boettcher³

*Theoretical Physics Institute, University of Alberta, Edmonton, Alberta T6G 2E1, Canada
and Department of Physics, University of Alberta, Edmonton, Alberta T6G 2E1, Canada*

 (Received 21 October 2023; revised 2 May 2024; accepted 26 June 2024; published 9 August 2024)

We study Anderson localization in disordered tight-binding models on hyperbolic lattices. Such lattices are geometries intermediate between ordinary two-dimensional crystalline lattices, which localize at infinitesimal disorder, and Bethe lattices, which localize at strong disorder. Using state-of-the-art computational group theory methods to create large systems, we approximate the thermodynamic limit through appropriate periodic boundary conditions and numerically demonstrate the existence of an Anderson localization transition on the $\{8,3\}$ and $\{8,8\}$ lattices. We find unusually large critical disorder strengths, determine critical exponents, and observe a strong finite-size effect in the level statistics.

DOI: 10.1103/PhysRevLett.133.066101

Introduction—Two-dimensional (2D) hyperbolic lattices with constant negative spatial curvature have recently been realized experimentally in circuit quantum electrodynamics (QED) [1], topoelectrical circuits [2–5], topological photonics [6], and scattering wave networks [7]. A hyperbolic $\{p, q\}$ lattice is a regular tiling of 2D hyperbolic space by p -sided polygonal faces and vertices of coordination number q , such that $(p-2)(q-2) > 4$. The scientific relevance of hyperbolic lattices ranges from testing fundamental principles such as the anti-de Sitter/conformal field theory correspondence in tabletop experiments [8–15], to applications in quantum computation [16–20] and quantum error correction [21–26]. As a new class of synthetic materials, they host a plethora of exotic physical properties beyond those identified in conventional Euclidean lattices, such as nontrivial crystalline symmetries [27–29], generalized Bloch states [30–37], modified role of interactions [38–40], unusual flat bands [41,42], and novel topological phenomena [3,5,29,43–49].

Inevitable in real experiments, disorder in lattice systems can be detrimental to the performance of quantum devices, but also lead to novel physical phenomena such as Anderson localization [50–52]. Prior investigations of disorder-induced localization primarily focused on tight-binding models on Euclidean lattices, where single-particle states in 2D become localized upon the presence of arbitrarily weak quenched disorder, an effect known as weak localization [53]. Anderson localization has also been studied for tight-binding models on treelike Bethe lattices [54–56] and random regular graphs [57–63], the latter being the finite-sized counterparts of the former with periodic boundary conditions. These lattices can be viewed

as the $p \rightarrow \infty$ limit of $\{p, q\}$ hyperbolic lattices [64] and exhibit a localization transition at finite disorder strength. Other non-Euclidean graphs exhibiting the Anderson localization transition include small-world networks [65,66] and Erdős-Rényi graphs [67–69].

Hyperbolic $\{p, q\}$ lattices with p finite are naturally considered two dimensional since they correspond to regular tilings of the 2D hyperbolic plane, as shown in Fig. 1(a). At the same time, much like Bethe lattices, the number of n walks starting from a given site grows exponentially with n . Thus, hyperbolic lattices share aspects of both conventional 2D lattices and treelike lattices. However, their localization properties under disorder are mostly uncharted. The robustness of certain topological features against disorder has been investigated in Refs. [43,44]. For continuum models, it has recently been argued that negative curvature prevents weak localization [70], hinting at the possibility of an Anderson transition in hyperbolic lattices.

In this Letter, we explicitly demonstrate the existence of an Anderson localization transition on hyperbolic lattices and characterize its properties. We first present a heuristic argument based on classical random walks that disordered hyperbolic $\{p, q\}$ lattices should exhibit a localization transition at a finite critical disorder strength. We then verify this hypothesis by numerical simulations of the Anderson model [Eq. (3)] on finite $\{8,3\}$ and $\{8,8\}$ lattices with up to $\mathcal{O}(10^4)$ sites and periodic boundary conditions (PBC). These so-called PBC clusters provide a reliable approximation of the infinite lattice and prevent spurious localization on the boundary, which, unlike a Euclidean boundary, would contain a macroscopic number of sites. We present our state-of-the-art technique for constructing large PBC clusters using computational group theory and benchmark it against the known thermodynamic-limit

*Contact author: anffany@ualberta.ca

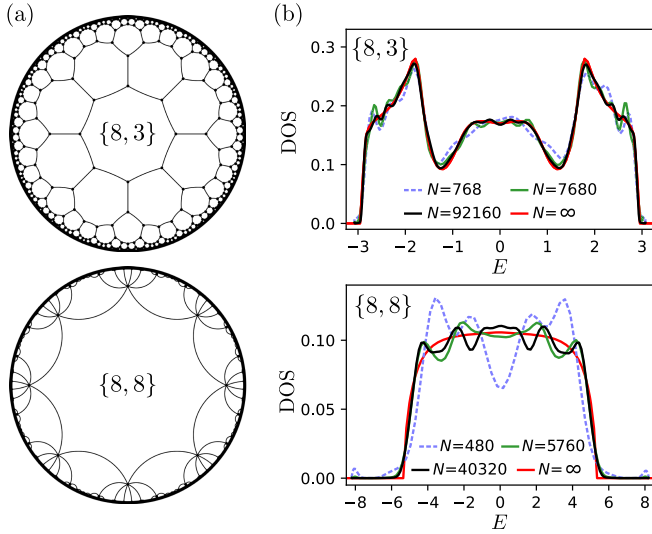


FIG. 1. Approaching the thermodynamic-limit with finite-sized hyperbolic lattices. (a) To study the localization phenomenon in hyperbolic space, we implement the Anderson model (3) on $\{8,3\}$ and $\{8,8\}$ hyperbolic lattices, here shown as embedded in the Poincaré disk. (b) To avoid boundary localization, we construct finite-sized hyperbolic lattices with periodic boundary conditions, dubbed PBC clusters. As system size N increases, the DOS of the disorder-free system ($u_i = 0$) on our PBC clusters converges to the thermodynamic-limit DOS. The latter (red curve) is captured accurately by the continued-fraction method [71].

density of states (DOS) in the disorder-free system. For the disordered system, we compute the level statistics and inverse participation ratio (IPR) averaged over many disorder realizations. We conduct a finite-size scaling analysis to determine, for the first time, the critical disorder strengths W_c and scaling length exponents ν on the $\{8,3\}$ and $\{8,8\}$ lattices. We find that $W_c/t \approx 15$ and 100, respectively, revealing that hyperbolic lattices are very robust toward disorder, in contrast to 2D Euclidean lattices that exhibit weak localization. Furthermore, we observe a strong finite-size effect in the level statistics, which is a key feature of localization in random regular graphs [57,58,61].

Random walks on hyperbolic lattices—We first argue that disordered hyperbolic lattices should exhibit a localization transition at a finite critical disorder strength based on the theory of random walks [72]. Starting at an arbitrary site, a random walker has an equal probability to proceed to each of its neighbors at each time step. By Pólya’s theorem [73], the expected number of returns (to the starting point) of a random walk in d -dimensional integer lattices \mathbb{Z}^d is infinite for $d \leq 2$ and finite for $d > 2$, implying that a Euclidean 1D or 2D random walk contains an infinite number of loops. These loops have crucial implications for transport properties, because the leading quantum correction to the Drude formula of conductivity is attributed to the quantum interference of clockwise and counterclockwise

electronic trajectories along each loop [74]. This so-called weak localization correction is large in 1D and 2D disordered Euclidean lattices, which greatly suppresses conduction. In contrast, we show below that the expected number of returns on a 2D hyperbolic $\{p,q\}$ lattice is finite, corresponding to only a small weak-localization correction. This is more akin to the 3D Euclidean case, which is known to display a localization transition [50].

Consider a random walk on an infinite $\{p,q\}$ lattice, starting at an arbitrary site i . The expected number of returns is $\mu = \sum_{n=0}^{\infty} P_n$, where P_n is the probability that an n -step walk (or n walk) starts and ends at site i (see Supplemental Material [75] for derivation). P_n is also the fractional of n cycles among all n walks. The total number of n walks is q^n . By graph theory, the number of n cycles based at site i is $(A^n)_{ii}$, with A the adjacency matrix of the infinite lattice. Diagonalizing A such that $A = \sum_a \lambda_a |\psi_a\rangle \langle \psi_a|$, we have $(A^n)_{ii} = \sum_a \lambda_a^n |\langle i|\psi_a\rangle|^2$, where $|i\rangle$ is the localized state at site i in the position basis. Denoting by $\lambda_r = \max_a |\lambda_a|$ the spectral radius of A , we then find

$$(A^n)_{ii} \leq \sum_a |\lambda_a|^n |\langle i|\psi_a\rangle|^2 \leq \lambda_r^n \sum_a |\langle i|\psi_a\rangle|^2 = \lambda_r^n. \quad (1)$$

The last equality follows from completeness of the $|\psi_a\rangle$ basis. Therefore, the fraction of n cycles is bounded from above according to $P_n = (A^n)_{ii}/q^n \leq (\lambda_r/q)^n$. Unlike in Euclidean lattices, the symmetry group of a hyperbolic $\{p,q\}$ lattice exhibits the mathematical property of non-amenability [81,82] and, as a result, its spectral radius λ_r is strictly less than q [64,83]. Hence, the expected number of returns,

$$\mu = \sum_{n=0}^{\infty} P_n \leq \sum_{n=0}^{\infty} \left(\frac{\lambda_r}{q}\right)^n = \frac{1}{1 - \lambda_r/q} < \infty, \quad (2)$$

is finite. This suggests that localization on disordered hyperbolic lattices occurs at a nonzero critical disorder strength.

Hyperbolic Anderson model—We formulate the Anderson model [50] on a hyperbolic $\{p,q\}$ lattice by the tight-binding Hamiltonian

$$H = -t \sum_{\langle i,j \rangle} (c_i^\dagger c_j + c_j^\dagger c_i) + \sum_i u_i c_i^\dagger c_i, \quad (3)$$

where c_i^\dagger (c_i) creates (annihilates) a particle on site i , t is the nearest-neighbor hopping amplitude, and the on-site potentials u_i are randomly drawn from a uniform distribution over the interval $[-(W/2), (W/2)]$. The Hamiltonian is motivated in part by the circuit QED experiments of Ref. [1], where $t \sim 100$ MHz and the on-site potentials have a mean value of 8 GHz with ~ 10 MHz variations. The realized system can thus be modeled by Eq. (3) with

$W/t \sim 0.1$. Henceforth, we set $t = 1$ and measure energies and W in units of t .

To demonstrate the localization transition on an infinite hyperbolic lattice and characterize its properties, we study the Hamiltonian (3) on large but finite lattices with PBC. Hyperbolic lattices with open boundary conditions, as shown in Fig. 1(a), are discussed, for instance, in Ref. [29]. Properly formulated PBC are essential in the hyperbolic context to systematically approach the thermodynamic limit, yet existing methods are limited either in the system size [84] or the number of realizations [85]. In this Letter, we propose a novel method which can produce unlimited realizations of hyperbolic PBC clusters with arbitrarily large system sizes. Moreover, the resulting clusters are defect-free systems with translation symmetry. To describe our method, we start by considering a finite patch of the infinite lattice and compactify it by identifying pairs of boundary edges, resulting in a tessellation of a high-genus Riemann surface [28,31,86]. The compactification is achieved through computing the quotient group $C = \Gamma/G$, where Γ is the translation symmetry group of the hyperbolic lattice and G is a normal subgroup of Γ (denoted $G \triangleleft \Gamma$). In other words, each element in Γ corresponds to a site in the infinite lattice, and G contains the equivalence relations which identify each site in the chosen patch with its (infinitely many) equivalent sites outside the patch. The normality constraint ensures that the cluster preserves a notion of translation symmetry and that no dislocations are introduced by the PBC. Each coset $[g] \in \Gamma/G$ represents a site in the PBC cluster, and two sites $[g_1], [g_2]$ are neighbors if $[g_1] = [g_2][\gamma_i]$ with γ_i a generator of Γ [31]. The number of cosets, i.e., the order of the group C , corresponds to the number of Bravais unit cells in the cluster, denoted by $N = |C|$.

However, not all choices of normal subgroup G give rise to PBC clusters that can correctly approximate the DOS in the thermodynamic limit [85,87]. For this, we have to construct a so-called *coherent sequence* of finite-index normal subgroups, $\{\tilde{G}_i\}$, such that $\tilde{G}_i \triangleleft \Gamma$ for all i and

$$\Gamma \triangleright \tilde{G}_1 \triangleright \tilde{G}_2 \triangleright \tilde{G}_3 \triangleright \dots \quad (4)$$

In addition, $\cap_{i=1}^{\infty} \tilde{G}_i = \{e\}$, where $\{e\}$ is the trivial group. Under these conditions, the PBC clusters $C_i = \Gamma/\tilde{G}_i$ approach the thermodynamic limit as i increases. We use the computational algebra software GAP [88,89] for generating finite coherent sequences through subgroup intersections of low-index normal subgroups [90,91] (see Ref. [75] for methods). We construct four finite coherent sequences of $\{8,8\}$ clusters with up to $N \sim 40\,000$ sites. By replacing each vertex of the $\{8,8\}$ cluster with a 16-site unit cell [28,75], this also yields coherent sequences of $\{8,3\}$ clusters with up to $N \sim 90\,000$ sites. The adjacency matrices of the generated clusters are available at [92]. Figure 1(b) shows the DOS of the disorder-free systems

obtained from our first PBC cluster sequence, computed with the kernel polynomial method [93] using the KWANT PYTHON package [94]. As the cluster size increases, the cluster DOS gradually approaches the thermodynamic limit [71] and more exact values of low DOS moments are reproduced (see Tables S2 and S3 of [75]), indicating convergence.

Having demonstrated that our sequences of PBC clusters accurately capture the thermodynamic limit in the clean limit, we next diagonalize the Anderson model (3) on $\{8,8\}$ clusters with $N = 100$ to $40\,320$ and $\{8,3\}$ clusters with $N = 160$ to $92\,160$. The single-particle Hamiltonian is given by the $N \times N$ adjacency matrix of the cluster (multiplied by -1) plus a diagonal matrix with random values in the range $[-(W/2), (W/2)]$. We consider 1000 to 100 000 disorder realizations, with more realizations for smaller clusters. For each realization, we use the Jacobi-Davidson algorithm through the software code of Ref. [95] to obtain the 20 eigenenergies E_α and eigenstates ψ_α closest to the center of the energy spectrum ($E = 0$ for the lattices considered here). We focus on such eigenstates because localization generally occurs first at the outer edges of the spectrum and gradually shifts toward the center as W increases, resulting in the so-called ‘‘mobility edge’’ structure in observables such as the IPR. Therefore, localization at $E \sim 0$ marks the localization phase transition. We verified that hyperbolic Anderson models indeed exhibit a mobility edge in the IPR.

Level statistics and inverse participation ratio—Level statistics, i.e., the distribution of consecutive gaps in an energy spectrum, offers critical insights into wave function localization [51,96,97]. Two delocalized wave functions are coupled due to their spatial overlaps, making degeneracy in their energy eigenvalues unfavorable due to level repulsion. As a result, the level statistics in the delocalized phase follows that of the Wigner-Dyson Gaussian orthogonal ensemble (GOE). In the localized phase, wave functions exhibit minimal overlap. Their energies are independent and resemble random values along a line, with level statistics described by the Poisson distribution.

For each cluster considered, we compute the level statistics of the Anderson model using the near-zero eigenvalues obtained above. Since the gaps between consecutive eigenvalues are strongly affected by the presence of finite-size-induced gaps, we circumvent this issue by considering the ratio of gaps in the sorted spectrum [98],

$$0 \leq r_\alpha = \frac{\min\{E_{\alpha+1} - E_\alpha, E_\alpha - E_{\alpha-1}\}}{\max\{E_{\alpha+1} - E_\alpha, E_\alpha - E_{\alpha-1}\}} \leq 1. \quad (5)$$

When binned into a histogram, r_α (compiled from different disorder realizations) follows a distribution that transitions from the Wigner surmise of GOE at small W to the Poisson distribution at large W [75]. This is most easily seen in the disorder-averaged expectation value $\langle r \rangle$, which changes

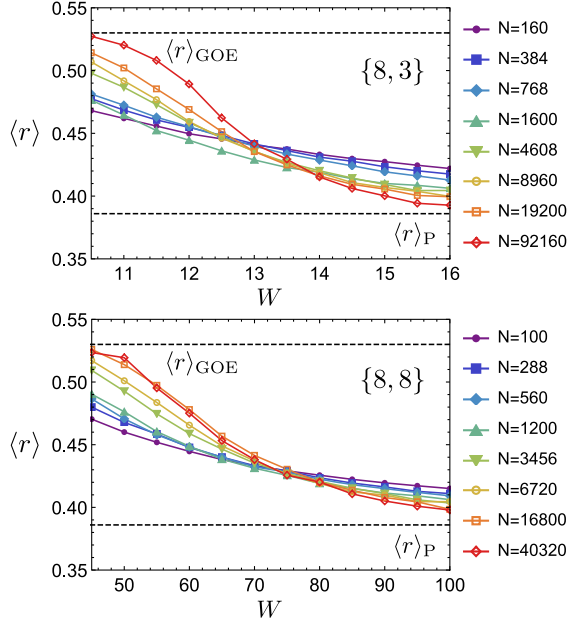


FIG. 2. Finite-size effect in the average gap ratio. The average gap ratio $\langle r \rangle$, averaged over disorder realizations and 20 eigenstates closest to energy $E = 0$, transitions from the GOE ensemble value $\langle r \rangle_{\text{GOE}} = 0.536$ to the Poissonian value $\langle r \rangle_{\text{P}} = 0.386$, which signals a localization transition. We observe a strong finite-size effect such that the pairwise crossing of the $\langle r \rangle$ curves drifts toward stronger W and $\langle r \rangle_{\text{P}}$ as system size N increases.

from the GOE value $\langle r \rangle_{\text{GOE}} = 4 - 2\sqrt{3} = 0.536$ [99] to the Poisson value $\langle r \rangle_{\text{P}} = 2 \ln 2 - 1 = 0.386$ upon increasing W (see Fig. 2 and Fig. S2 of [75]), signaling a localization transition.

The value $\langle r \rangle$ at the critical disorder W_c is typically independent of N for Euclidean systems, albeit dependent on the boundary condition [51], so the intersection of $\langle r \rangle$ curves can be used to locate the critical point. However, here we observe a strong finite-size effect such that the intersection of $\langle r \rangle$ curves drifts toward stronger W and $\langle r \rangle_{\text{P}}$ as N increases, as shown in Fig. 2. Such crossing drift has also been observed in the Anderson model on the $\{\infty, 3\}$ lattices [57,58,61]. We extrapolate the disorder strength at the intersection, denoted W^* , to the infinite- N limit using the model $W^* = W_c - \beta / \ln(N)$ for some fitting parameter β and determine $W_c \sim 15$ and 100 for $\{8,3\}$ and $\{8,8\}$ [75].

The IPR of a normalized wave function $\psi(z)$ is given by

$$\mathcal{I}(\psi) = \sum_{i=1}^N |\psi(z_i)|^4, \quad (6)$$

where z_i denote the site coordinates. If ψ is highly delocalized with finite support on all sites, then $|\psi(z_i)|^2 \rightarrow 0$ as $N \rightarrow \infty$, leading to $\mathcal{I}(\psi_{\text{deloc}}) \rightarrow 0$. At the other extreme, if ψ is localized on a single site j such that $|\psi(z_i)|^2 \sim \delta_{ij}$, then $\mathcal{I}(\psi_{\text{loc}}) \sim 1$. We compute \mathcal{I} for all $E \approx 0$ eigenstates

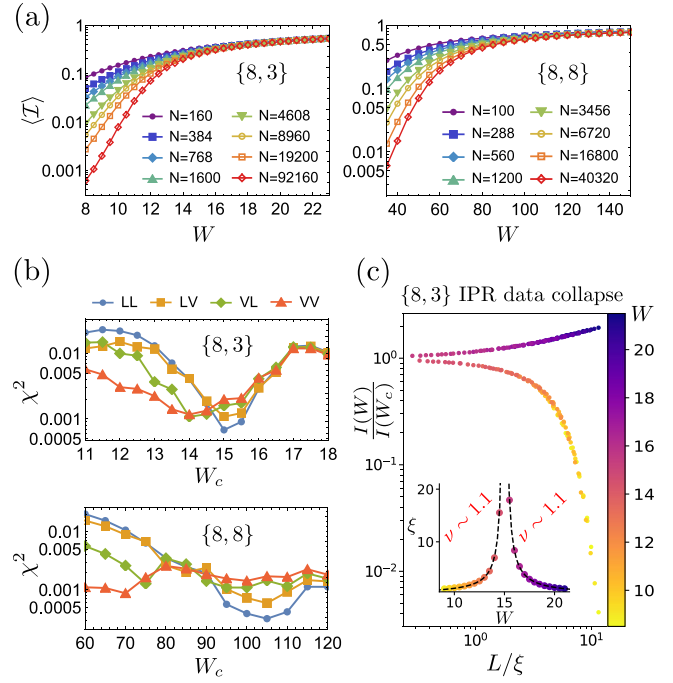


FIG. 3. Finite-size scaling analysis of IPR. (a) $\langle \mathcal{I} \rangle$ data used for the finite-size scaling analysis. (b) Assuming linear scaling behavior as in Eq. (7) yields the optimal data collapse on both the delocalized and localized sides of the transition. This is indicated by the minimal χ^2 values, where we denote LL: linear-linear, LV: linear-volumetric, etc., according to the scaling law used on either side of the transition. The best data collapse occurs at $W_c \approx 15$ for $\{8,3\}$ and $W_c \approx 100$ for $\{8,8\}$. (c) The collapsed IPR data of the $\{8,3\}$ model (see Fig. S5 of [75] for other collapses). The associated scaling length follows $\xi(W) \propto |W - W_c|^{-\nu}$ with critical exponent ν as indicated.

obtained above, which are then averaged over disorder realizations. We find that the disorder-averaged $\langle \mathcal{I} \rangle$ for the Anderson model on various PBC clusters increase from small values to ~ 1 at large disorder, suggesting a localization transition for both $\{8,3\}$ and $\{8,8\}$ lattices. Figure 3(a) shows the $\langle \mathcal{I} \rangle$ data used to conduct the following finite-size scaling analysis.

Finite-size scaling and critical properties—Having established the localization transition on hyperbolic lattices, we now use finite-size scaling to extract its critical properties, including the critical disorder strength and critical exponents. We follow Ref. [66] to conduct the finite-size scaling analysis of the observables $\eta(W, N) \equiv (\langle r \rangle - \langle r \rangle_{\text{P}}) / (\langle r \rangle_{\text{GOE}} - \langle r \rangle_{\text{P}})$ and $\mathcal{I}(W, N) \equiv \langle \mathcal{I} \rangle$ (see Ref. [75] for methods). The exponential growth of system size N of hyperbolic and Bethe lattices with graph diameter L , i.e., $N \sim e^{cL}$ for some lattice-dependent constant c , suggests two potential scaling laws for a given observable O . Either we have

$$O(W, N) = O(W_c, N) F_{\text{lin}}(L/\xi(W)), \quad (7)$$

with an unknown scaling function $F_{\text{lin}}(L/\xi(W))$ and scaling length $\xi(W)$, or

$$O(W, N) = O(W_c, N)F_{\text{vol}}(N/\Lambda(W)), \quad (8)$$

with scaling function $F_{\text{vol}}(N/\Lambda(W))$ and scaling volume $\Lambda(W)$. We refer to the two cases as linear and volumetric scaling, respectively. For d -dimensional Euclidean lattices, the two scaling behaviors are equivalent due to $N/\Lambda = (L/\xi)^d$. In contrast, in hyperbolic and Bethe lattices, the ratio $N/\Lambda = e^{c(L-\xi)}$ is a function of $L - \xi$ instead of L/ξ . Therefore, we must examine both scaling laws separately and identify which one applies to the data. In the following we omit the lattice-dependent constant c and let $L = \log(N)$.

We prepare curves of $\eta(W, N)$ and $I(W, N)$ as functions of N , each curve at a fixed W . We then make assumptions on the critical disorder W_c and the scaling behaviors (either linear or volumetric) on the delocalized and localized sides of the transition. According to the scaling laws in Eqs. (7) and (8), all curves rescaled by the critical curve, i.e., $O(W, N)/O(W_c, N)$, should collapse into a single scaling function. The quality of the collapse is measured by the least χ^2 , indicating an optimal assumption about W_c and the scaling behaviors.

As shown in Fig. 3(b), the χ^2 obtained from collapsing $I(W, N)$ reveals a clear local minimum at $W_c \sim 15(100)$ for $\{8,3\}$ ($\{8,8\}$), consistent with the crossing-drift analysis. We find that the χ^2 obtained from collapsing $\eta(W, N)$ is less informative due to noise in the level statistics data [75]. Linear scaling of $I(W, N)$ in the vicinity of the transition gives the best data collapse on both the delocalized and localized sides. However, since we only consider system sizes up to $\sim 100\,000$, our result does not exclude the possibility of volumetric scaling for larger systems. Such finite-size crossover has been observed in the Anderson model on random regular graphs [57], such that the delocalized phase is characterized by a correlation volume $N_c(W)$, separating smaller systems $N < N_c(W)$ with linear scaling and larger systems $N > N_c(W)$ with volumetric scaling.

The critical points of $\{\infty, 3\}$ and $\{\infty, 8\}$ Anderson models have been estimated at $W_c \approx 18$ [54,59,60,63] and $W_c \sim 110$ [62], respectively. Comparing the four lattices $\{8,3\}$, $\{\infty, 3\}$, $\{8,8\}$, and $\{\infty, 8\}$, we find that the critical disorder W_c increases with the magnitude of the lattice curvature in units of the lattice constant, which is 0.73, 1.10, 3.06, and 3.23, respectively [29]. This can be attributed to negative curvature acting as an infrared regulator that suppresses the usual logarithmic divergence in the weak-localization correction in 2D [70,100]. This suppression is more effective for stronger curvature, yielding a higher threshold to observe localization.

Assuming the linear-linear scaling law and $W_c \sim 15(100)$ for $\{8,3\}$ ($\{8,8\}$), we plot the collapsed η and I data

[Fig. 3(c) and Fig. S5 of [75]] and determine the scaling length exponent ν by fitting $\xi \propto |W - W_c|^{-\nu}$ to find $(\nu_{\eta, \text{deloc}}^{\{8,3\}}, \nu_{\eta, \text{loc}}^{\{8,3\}}) \approx (0.5, 0.4)$, $(\nu_{\eta, \text{deloc}}^{\{8,8\}}, \nu_{\eta, \text{loc}}^{\{8,8\}}) \approx (0.9, 0.9)$, $(\nu_{I, \text{deloc}}^{\{8,3\}}, \nu_{I, \text{loc}}^{\{8,3\}}) \approx (1.1, 1.1)$, $(\nu_{I, \text{deloc}}^{\{8,8\}}, \nu_{I, \text{loc}}^{\{8,8\}}) \approx (1.1, 0.9)$ on the delocalized and localized sides, respectively. For comparison, the corresponding critical exponents on random regular graphs and small-world networks with average coordination number of 3 are known to be $(\nu_{\eta, \text{deloc}}^{\{\infty, 3\}}, \nu_{\eta, \text{loc}}^{\{\infty, 3\}}) \approx (0.5, 0.5)$ and $(\kappa_{I, \text{deloc}}^{\{\infty, 3\}}, \nu_{I, \text{loc}}^{\{\infty, 3\}}) \approx (0.5, 1)$, where $\kappa_{I, \text{deloc}}^{\{\infty, 3\}}$ is the critical exponent of the scaling volume [59,65–67]. We also found that the IPR at criticality follows the multifractal scaling $I(W_c) \propto L^{-\tau_2}$ with fractal dimension $\tau_2^{\{8,3\}} \sim 0.3$ and $\tau_2^{\{8,8\}} \sim 0.2$ [75].

Conclusion—In this Letter, we have studied, for the first time, the Anderson localization transition on hyperbolic $\{p, q\}$ lattices. To eliminate boundary influence while preserving hyperbolic translation symmetry in the clean limit, we developed an efficient method to create large PBC clusters. We benchmarked the disorder-free system against the known thermodynamic limit and found very good agreement for large systems with $\mathcal{O}(10^4)$ sites and adequate agreement even with $\mathcal{O}(10^2)$ sites. Through analyzing the level statistics and IPR of the Anderson models, we determined the critical disorder strengths on the $\{8,3\}$ and $\{8,8\}$ lattices to be $W_c \approx 15t$ and $100t$, respectively, implying high resilience against disorder on hyperbolic lattices. This understanding is instrumental in circuit QED applications, where small variations in on-site potentials lead to disorders with W comparable to t . We revealed that hyperbolic lattices are genuinely distinct from 2D Euclidean lattices, which exhibit the localization of all eigenstates at infinitesimal disorder strength. Furthermore, they suffer from a strong finite-size effect near the localization transition. In particular, the pairwise intersection of $\langle r \rangle$ curves drifts toward strong disorder and the Poisson distribution, as also seen in the Anderson models on Bethe lattices and random regular graphs. Our results pave the way for future studies of hyperbolic localization.

The localization of wave functions can be realized experimentally in (otherwise clean) topoelectrical circuits through creating artificial variation in local resistance. Besides localization, our PBC clusters, accessible at Ref. [92], are a powerful tool for various numerical studies of hyperbolic lattices. On the one hand, they are crucial for investigating bulk physics by emulating the thermodynamic limit while eliminating boundary effects. On the other hand, by introducing suitable vacancies, one can design a controlled study of the hyperbolic boundary, or defects in general, to test the bulk-boundary correspondence and emergent boundary phenomena.

Acknowledgments—We thank Jonathan Curtis, Victor Galitski, Alexey Gorshkov, and Canon Sun for valuable

discussions. This research was enabled in part by support provided by Compute Ontario and the Digital Research Alliance of Canada. A. C. was supported by the Avadh Bhatia Fellowship at the University of Alberta. A. C. and I. B. acknowledge support through the University of Alberta startup fund UOFAB Startup Boettcher. J. M. was supported by NSERC Discovery Grants No. RGPIN-2020-06999 and No. RGPAS-2020-00064; the Canada Research Chair (CRC) Program; the Government of Alberta's Major Innovation Fund (MIF); and the Pacific Institute for the Mathematical Sciences (PIMS) Collaborative Research Group program. I. B. acknowledges funding from the NSERC Discovery Grants No. RGPIN-2021-02534 and No. DGECR2021-00043.

- [1] A. J. Kollár, M. Fitzpatrick, and A. A. Houck, Hyperbolic lattices in circuit quantum electrodynamics, *Nature (London)* **571**, 45 (2019).
- [2] P. M. Lenggenhager, A. Stegmaier, L. K. Upreti, T. Hofmann, T. Helbig, A. Vollhardt, M. Greiter, C. H. Lee, S. Imhof, H. Brand, T. Kießling, I. Boettcher, T. Neupert, R. Thomale, and T. Bzdušek, Simulating hyperbolic space on a circuit board, *Nat. Commun.* **13**, 4373 (2022).
- [3] W. Zhang, H. Yuan, N. Sun, H. Sun, and X. Zhang, Observation of novel topological states in hyperbolic lattices, *Nat. Commun.* **13**, 2937 (2022).
- [4] A. Chen, H. Brand, T. Helbig, T. Hofmann, S. Imhof, A. Fritzsche, T. Kießling, A. Stegmaier, L. K. Upreti, T. Neupert, T. Bzdušek, M. Greiter, R. Thomale, and I. Boettcher, Hyperbolic matter in electrical circuits with tunable complex phases, *Nat. Commun.* **14**, 622 (2023).
- [5] W. Zhang, F. Di, X. Zheng, H. Sun, and X. Zhang, Hyperbolic band topology with non-trivial second Chern numbers, *Nat. Commun.* **14**, 1083 (2023).
- [6] L. Huang, L. He, W. Zhang, H. Zhang, D. Liu, X. Feng, F. Liu, K. Cui, Y. Huang, W. Zhang, and X. Zhang, Hyperbolic photonic topological insulators, *Nat. Commun.* **15**, 1647 (2024).
- [7] Q. Chen, Z. Zhang, H. Qin, A. Bossart, Y. Yang, H. Chen, and R. Fleury, Anomalous and Chern topological waves in hyperbolic networks, *Nat. Commun.* **15**, 2293 (2024).
- [8] L. Boyle, M. Dickens, and F. Flicker, Conformal quasicrystals and holography, *Phys. Rev. X* **10**, 011009 (2020).
- [9] M. Asaduzzaman, S. Catterall, J. Hubisz, R. Nelson, and J. Unmuth-Yockey, Holography on tessellations of hyperbolic space, *Phys. Rev. D* **102**, 034511 (2020).
- [10] R. C. Brower, C. V. Cofburn, A. L. Fitzpatrick, D. Howarth, and C.-I. Tan, Lattice setup for quantum field theory in AdS₂, *Phys. Rev. D* **103**, 094507 (2021).
- [11] P. Basteiro, F. Dusel, J. Erdmenger, D. Herdt, H. Hinrichsen, R. Meyer, and M. Schrauth, Breitenlohner-Freedman bound on hyperbolic tilings, *Phys. Rev. Lett.* **130**, 091604 (2023).
- [12] P. Basteiro, G. D. Giulio, J. Erdmenger, J. Karl, R. Meyer, and Z.-Y. Xian, Towards explicit discrete holography: Aperiodic spin chains from hyperbolic tilings, *SciPost Phys.* **13**, 103 (2022).
- [13] P. Basteiro, R. N. Das, G. Di Giulio, and J. Erdmenger, Aperiodic spin chains at the boundary of hyperbolic tilings, *SciPost Phys.* **15**, 218 (2023).
- [14] J. Chen, F. Chen, Y. Yang, L. Yang, Z. Chen, Y. Meng, B. Yan, X. Xi, Z. Zhu, G.-G. Liu, P. P. Shum, H. Chen, R.-G. Cai, R.-Q. Yang, Y. Yang, and Z. Gao, AdS/CFT correspondence in hyperbolic lattices, [arXiv:2305.04862](https://arxiv.org/abs/2305.04862).
- [15] S. Dey, A. Chen, P. Basteiro, A. Fritzsche, M. Greiter, M. Kaminski, P. M. Lenggenhager, R. Meyer, R. Sorbello, A. Stegmaier, R. Thomale, J. Erdmenger, and I. Boettcher, Simulating holographic conformal field theories on hyperbolic lattices, [arXiv:2404.03062](https://arxiv.org/abs/2404.03062).
- [16] G. Vidal, Entanglement renormalization, *Phys. Rev. Lett.* **99**, 220405 (2007).
- [17] G. Vidal, Class of quantum many-body states that can be efficiently simulated, *Phys. Rev. Lett.* **101**, 110501 (2008).
- [18] B. Swingle, Entanglement renormalization and holography, *Phys. Rev. D* **86**, 065007 (2012).
- [19] J. Haegeman, T. J. Osborne, H. Verschelde, and F. Verstraete, Entanglement renormalization for quantum fields in real space, *Phys. Rev. Lett.* **110**, 100402 (2013).
- [20] N. Bao, C. J. Cao, S. M. Carroll, and A. Chatwin-Davies, de Sitter space as a tensor network: Cosmic no-hair, complementarity, and complexity, *Phys. Rev. D* **96**, 123536 (2017).
- [21] F. Pastawski, B. Yoshida, D. Harlow, and J. Preskill, Holographic quantum error-correcting codes: Toy models for the bulk/boundary correspondence, *J. High Energy Phys.* **06** (2015) 149.
- [22] N. P. Breuckmann and B. M. Terhal, Constructions and noise threshold of hyperbolic surface codes, *IEEE Trans. Inf. Theory* **62**, 3731 (2016).
- [23] N. P. Breuckmann, C. Vuillot, E. Campbell, A. Krishna, and B. M. Terhal, Hyperbolic and semi-hyperbolic surface codes for quantum storage, *Quantum Sci. Technol.* **2**, 035007 (2017).
- [24] A. Lavasani, G. Zhu, and M. Barkeshli, Universal logical gates with constant overhead: Instantaneous Dehn twists for hyperbolic quantum codes, *Quantum* **3**, 180 (2019).
- [25] A. Jahn and J. Eisert, Holographic tensor network models and quantum error correction: A topical review, *Quantum Sci. Technol.* **6**, 033002 (2021).
- [26] A. Fahimniya, H. Dehghani, K. Bharti, S. Mathew, A. J. Kollár, A. V. Gorshkov, and M. J. Gullans, Fault-tolerant hyperbolic Floquet quantum error correcting codes, [arXiv:2309.10033](https://arxiv.org/abs/2309.10033).
- [27] I. Boettcher, P. Bienias, R. Belyansky, A. J. Kollár, and A. V. Gorshkov, Quantum simulation of hyperbolic space with circuit quantum electrodynamics: From graphs to geometry, *Phys. Rev. A* **102**, 032208 (2020).
- [28] I. Boettcher, A. V. Gorshkov, A. J. Kollár, J. Maciejko, S. Rayan, and R. Thomale, Crystallography of hyperbolic lattices, *Phys. Rev. B* **105**, 125118 (2022).
- [29] A. Chen, Y. Guan, P. M. Lenggenhager, J. Maciejko, I. Boettcher, and T. Bzdušek, Symmetry and topology of hyperbolic Haldane models, *Phys. Rev. B* **108**, 085114 (2023).
- [30] J. Maciejko and S. Rayan, Hyperbolic band theory, *Sci. Adv.* **7**, eabe9170 (2021).

- [31] J. Maciejko and S. Rayan, Automorphic Bloch theorems for hyperbolic lattices, *Proc. Natl. Acad. Sci. U.S.A.* **119**, e2116869119 (2022).
- [32] N. Cheng, F. Serafin, J. McInerney, Z. Rocklin, K. Sun, and X. Mao, Band theory and boundary modes of high-dimensional representations of infinite hyperbolic lattices, *Phys. Rev. Lett.* **129**, 088002 (2022).
- [33] P. M. Lenggenhager, J. Maciejko, and T. Bzdušek, Non-Abelian hyperbolic band theory from supercells, *Phys. Rev. Lett.* **131**, 226401 (2023).
- [34] G. Shankar and J. Maciejko, Hyperbolic lattices and two-dimensional Yang-Mills theory, [arXiv:2309.03857](https://arxiv.org/abs/2309.03857).
- [35] E. Kienzle and S. Rayan, Hyperbolic band theory through Higgs bundles, *Adv. Math.* **409**, 108664 (2022).
- [36] Á. Nagy and S. Rayan, On the hyperbolic Bloch transform, *Ann. Henri Poincaré* **25**, 1713 (2024).
- [37] E. Petermann and H. Hinrichsen, Eigenmodes of the laplacian on hyperbolic lattices, *Phys. Rev. D* **109**, 106019 (2024).
- [38] P. Bienias, I. Boettcher, R. Belyansky, A. J. Kollár, and A. V. Gorshkov, Circuit quantum electrodynamics in hyperbolic space: From photon bound states to frustrated spin models, *Phys. Rev. Lett.* **128**, 013601 (2022).
- [39] N. Gluscevich, A. Samanta, S. Manna, and B. Roy, Dynamic mass generation on two-dimensional electronic hyperbolic lattices, [arXiv:2302.04864](https://arxiv.org/abs/2302.04864).
- [40] N. Gluscevich and B. Roy, Magnetic catalysis in weakly interacting hyperbolic Dirac materials, [arXiv:2305.11174](https://arxiv.org/abs/2305.11174).
- [41] T. Bzdušek and J. Maciejko, Flat bands and band-touching from real-space topology in hyperbolic lattices, *Phys. Rev. B* **106**, 155146 (2022).
- [42] R. Mosseri, R. Vogeler, and J. Vidal, Aharonov-Bohm cages, flat bands, and gap labeling in hyperbolic tilings, *Phys. Rev. B* **106**, 155120 (2022).
- [43] S. Yu, X. Piao, and N. Park, Topological hyperbolic lattices, *Phys. Rev. Lett.* **125**, 053901 (2020).
- [44] D. M. Urwyler, P. M. Lenggenhager, I. Boettcher, R. Thomale, T. Neupert, and T. Bzdušek, Hyperbolic topological band insulators, *Phys. Rev. Lett.* **129**, 246402 (2022).
- [45] Z.-R. Liu, C.-B. Hua, T. Peng, and B. Zhou, Chern insulator in a hyperbolic lattice, *Phys. Rev. B* **105**, 245301 (2022).
- [46] Z.-R. Liu, C.-B. Hua, T. Peng, R. Chen, and B. Zhou, Higher-order topological insulators in hyperbolic lattices, *Phys. Rev. B* **107**, 125302 (2023).
- [47] Q. Pei, H. Yuan, W. Zhang, and X. Zhang, Engineering boundary-dominated topological states in defective hyperbolic lattices, *Phys. Rev. B* **107**, 165145 (2023).
- [48] Y.-L. Tao and Y. Xu, Higher-order topological hyperbolic lattices, *Phys. Rev. B* **107**, 184201 (2023).
- [49] T. Tummuru, A. Chen, P. M. Lenggenhager, T. Neupert, J. Maciejko, and T. Bzdušek, Hyperbolic non-Abelian semimetal, *Phys. Rev. Lett.* **132**, 206601 (2024).
- [50] P. W. Anderson, Absence of diffusion in certain random lattices, *Phys. Rev.* **109**, 1492 (1958).
- [51] F. Evers and A. D. Mirlin, Anderson transitions, *Rev. Mod. Phys.* **80**, 1355 (2008).
- [52] A. Lagendijk, B. Tiggelen, and D. Wiersma, Fifty years of Anderson localization, *Phys. Today* **62**, No. 8, 24 (2009).
- [53] G. Bergmann, Weak localization in thin films: A time-of-flight experiment with conduction electrons, *Phys. Rep.* **107**, 1 (1984).
- [54] R. Abou-Chacra, D. J. Thouless, and P. W. Anderson, A self-consistent theory of localization, *J. Phys. C* **6**, 1734 (1973).
- [55] R. Abou-Chacra and D. J. Thouless, Self-consistent theory of localization. II. Localization near the band edges, *J. Phys. C* **7**, 65 (1974).
- [56] A. D. Mirlin and Y. V. Fyodorov, Localization transition in the Anderson model on the Bethe lattice: Spontaneous symmetry breaking and correlation functions, *Nucl. Phys. B* **366**, 507 (1991).
- [57] K. S. Tikhonov, A. D. Mirlin, and M. A. Skvortsov, Anderson localization and ergodicity on random regular graphs, *Phys. Rev. B* **94**, 220203(R) (2016).
- [58] G. Biroli and M. Tarzia, Delocalization and ergodicity of the Anderson model on Bethe lattices, [arXiv:1810.07545](https://arxiv.org/abs/1810.07545).
- [59] K. S. Tikhonov and A. D. Mirlin, Critical behavior at the localization transition on random regular graphs, *Phys. Rev. B* **99**, 214202 (2019).
- [60] G. Parisi, S. Pascazio, F. Pietracaprina, V. Ros, and A. Scardicchio, Anderson transition on the bethe lattice: An approach with real energies, *J. Phys. A* **53**, 014003 (2019).
- [61] K. Tikhonov and A. Mirlin, From Anderson localization on random regular graphs to many-body localization, *Ann. Phys. (Amsterdam)* **435**, 168525 (2021).
- [62] J.-N. Herre, J. F. Karcher, K. S. Tikhonov, and A. D. Mirlin, Ergodicity-to-localization transition on random regular graphs with large connectivity and in many-body quantum dots, *Phys. Rev. B* **108**, 014203 (2023).
- [63] P. Sierant, M. Lewenstein, and A. Scardicchio, Universality in Anderson localization on random graphs with varying connectivity, *SciPost Phys.* **15**, 045 (2023).
- [64] A. J. Kollár, M. Fitzpatrick, P. Sarnak, and A. A. Houck, Line-graph lattices: Euclidean and non-Euclidean flat bands, and implementations in circuit quantum electrodynamics, *Commun. Math. Phys.* **376**, 1909 (2020).
- [65] I. Garcia-Mata, O. Giraud, B. Georgeot, J. Martin, R. Dubertrand, and G. Lemarié, Scaling theory of the Anderson transition in random graphs: Ergodicity and universality, *Phys. Rev. Lett.* **118**, 166801 (2017).
- [66] I. Garcia-Mata, J. Martin, O. Giraud, B. Georgeot, R. Dubertrand, and G. Lemarié, Critical properties of the Anderson transition on random graphs: Two-parameter scaling theory, Kosterlitz-Thouless type flow, and many-body localization, *Phys. Rev. B* **106**, 214202 (2022).
- [67] M. Sade, T. Kalisky, S. Havlin, and R. Berkovits, Localization transition on complex networks via spectral statistics, *Phys. Rev. E* **72**, 066123 (2005).
- [68] H. J. Mard, J. A. Hoyos, E. Miranda, and V. Dobrosavljević, Strong-disorder approach for the Anderson localization transition, *Phys. Rev. B* **96**, 045143 (2017).
- [69] J. Alt, R. Ducatez, and A. Knowles, Delocalization transition for critical Erdős-Rényi graphs, *Commun. Math. Phys.* **388**, 507 (2021).
- [70] J. B. Curtis, P. Narang, and V. Galitski, Absence of weak localization on negative curvature surfaces, [arXiv:2308.01351](https://arxiv.org/abs/2308.01351).

- [71] R. Mosseri and J. Vidal, Density of states of tight-binding models in the hyperbolic plane, *Phys. Rev. B* **108**, 035154 (2023).
- [72] A. Einstein, Über die von der molekularkinetischen Theorie der Wärme geforderte Bewegung von in ruhenden Flüssigkeiten suspendierten Teilchen, *Ann. Phys. (N.Y.)* **322**, 549 (1905).
- [73] G. Pólya, Über eine Aufgabe der Wahrscheinlichkeitsrechnung betreffend die Irrfahrt im Straßennetz, *Math. Ann.* **84**, 149 (1921).
- [74] S. Datta, *Electronic Transport in Mesoscopic Systems* (Cambridge University Press, Cambridge, England, 1995), 10.1017/CBO9780511805776.
- [75] See Supplemental Material at <http://link.aps.org/supplemental/10.1103/PhysRevLett.133.066101>, which cites additional Refs. [76–80], for details on the construction of the PBC clusters and the finite-size scaling analyses.
- [76] R. Aurich, E. Bogomolny, and F. Steiner, Periodic orbits on the regular hyperbolic octagon, *Physica (Amsterdam)* **48D**, 91 (1991).
- [77] J. Bolte, Some studies on arithmetical chaos in classical and quantum mechanics, *Int. J. Mod. Phys. B* **07**, 4451 (1993).
- [78] E. Bogomolny, B. Georgeot, M.-J. Giannoni, and C. Schmit, Arithmetical chaos, *Phys. Rep.* **291**, 219 (1997).
- [79] A. Attar and I. Boettcher, Selberg trace formula in hyperbolic band theory, *Phys. Rev. E* **106**, 034114 (2022).
- [80] S. Katok, *Fuchsian Groups* (The University of Chicago Press, Chicago, 1992).
- [81] H. Kesten, Symmetric random walks on groups, *Trans. Am. Math. Soc.* **92**, 336 (1959).
- [82] R. Brooks, Amenability and the spectrum of the Laplacian, *Bull. Am. Math. Soc.* **6**, 87 (1982).
- [83] W. Woess, *Random Walks on Infinite Graphs and Groups* (Cambridge University Press, Cambridge, England, 2000).
- [84] M. Conder, Quotients of triangle groups acting on surfaces of genus 2 to 101, <https://www.math.auckland.ac.nz/~conder/TriangleGroupQuotients101.txt> (2007) [Online; accessed 01-October-2023].
- [85] F. R. Lux and E. Prodan, Spectral and combinatorial aspects of Cayley-crystals, *Ann. Henri Poincaré* (2023).
- [86] A. Stegmaier, L. K. Upreti, R. Thomale, and I. Boettcher, Universality of Hofstadter butterflies on hyperbolic lattices, *Phys. Rev. Lett.* **128**, 166402 (2022).
- [87] F. R. Lux and E. Prodan, Converging periodic boundary conditions and detection of topological gaps on regular hyperbolic tessellations, *Phys. Rev. Lett.* **131**, 176603 (2023).
- [88] F. Rober, The GAP package LINS, <https://github.com/FriedrichRober/LINS> (2020).
- [89] GAP, GAP—Groups, Algorithms, and Programming, Version 4.11.1, The GAP Group (2021), <https://www.gap-system.org>.
- [90] D. Firth, An algorithm to find normal subgroups of a finitely presented group, up to a given finite index, Ph.D. thesis, University of Warwick, 2004.
- [91] M. Conder and P. Dobcsányi, Applications and adaptations of the low index subgroups procedure, *Math. Comp.* **74**, 485 (2005).
- [92] A. Chen, J. Maciejko, and I. Boettcher, Supplemental Data for: Anderson localization transition in disordered hyperbolic lattices (2024).
- [93] A. Weiße, G. Wellein, A. Alvermann, and H. Fehske, The kernel polynomial method, *Rev. Mod. Phys.* **78**, 275 (2006).
- [94] C. W. Groth, M. Wimmer, A. R. Akhmerov, and X. Waintal, Kwant: A software package for quantum transport, *New J. Phys.* **16**, 063065 (2014).
- [95] M. Bollhöfer and Y. Notay, JADAMILU: A software code for computing selected eigenvalues of large sparse symmetric matrices, *Comput. Phys. Commun.* **177**, 951 (2007).
- [96] B. I. Shklovskii, B. Shapiro, B. R. Sears, P. Lambrianides, and H. B. Shore, Statistics of spectra of disordered systems near the metal-insulator transition, *Phys. Rev. B* **47**, 11487 (1993).
- [97] A. D. Mirlin, Statistics of energy levels and eigenfunctions in disordered systems, *Phys. Rep.* **326**, 259 (2000).
- [98] V. Oganesyan and D. A. Huse, Localization of interacting fermions at high temperature, *Phys. Rev. B* **75**, 155111 (2007).
- [99] Y. Y. Atas, E. Bogomolny, O. Giraud, and G. Roux, Distribution of the ratio of consecutive level spacings in random matrix ensembles, *Phys. Rev. Lett.* **110**, 084101 (2013).
- [100] C. G. Callan and F. Wilczek, Infrared behavior at negative curvature, *Nucl. Phys.* **B340**, 366 (1990).